

Enhancing Cognitive Radio Systems with Robust Reasoning

Evgenia Adamopoulou¹, Konstantinos Demestichas¹, Panagiotis Demestichas², and Michael Theologou¹

¹National Technical University of Athens, Athens, Greece, eadam@cn.ntua.gr, cdemest@cn.ntua.gr

²University of Piraeus, Piraeus, Greece

Abstract—Cognitive radio systems dynamically reconfigure the algorithms and parameters they use, in order to adapt to the changing environment conditions. However, reaching proper reconfiguration decisions presupposes a way of knowing, with high enough assurance, the capabilities of the alternate configurations, especially in terms of achievable transmission capacity and coverage. The present paper addresses this problem, firstly, by specifying a complete process for extracting estimations of the capabilities of candidate configurations, in terms of transmission capacity and coverage, and, secondly, by enhancing these estimations with the employment of a machine learning technique. The technique is based on the use of Bayesian Networks, in conjunction with an effective learning and adaptation strategy, and aims at extracting and exploiting knowledge and experience, in order to reach robust (i.e., stable and reliable) estimations of the configurations' capabilities. Comprehensive results of the proposed method are presented, in order to validate its functionality.

Index Terms—Bayesian networks, Cognitive radio, Interference sensing, Machine learning, Reasoning.

I. INTRODUCTION

TODAY'S wireless access scenery comprises various heterogeneous technologies: 2G, 2.5G and 3G cellular systems (e.g., GSM, GPRS, UMTS), wireless local and metropolitan area networks, as well as broadcast networks, such as Digital Audio Broadcasting (DAB) and Digital Video Broadcasting (DVB). The evolution of the above mentioned wireless communication systems, over the past years, demonstrates a clear trend towards architectures that will support multiple access technologies, and multimode mobile terminal devices, i.e. capable of alternately operating in the diverse radio segments available in the infrastructure.

This trend is often referred to as 'systems beyond 3G' (B3G), and its main notion is that a network operator can rely on multiple Radio Access Technologies (RATs) for achieving the desired Quality of Service (QoS), i.e. performance (e.g., bit-rate, delay, jitter), availability (blocking probability), reliability (e.g., handover blocking probability), as well as

security/privacy, in a cost-efficient manner [1]-[4]. The need for this stems from the fact that each RAT is best suited for handling certain – but not all – situations, especially in terms of desirable transmission capacity, coverage, mobility support and cost. Thus, in order to be competitive and raise customer satisfaction, a network operator will need to combine the benefits offered by different RATs.

Although significant steps have been made towards the joint utilization of the heterogeneous access technologies, the primary resource that all wireless technologies are built upon, i.e. the electromagnetic radio spectrum, is limited by its nature. Moreover, its fragmentation into separate frequency bands has resulted in the over-utilization of some of them, while others remain largely unoccupied [5]-[7]. The underutilization of radio spectrum is the result of a number of different factors including overly conservative allocation of guard bands; a migration from spectrally inefficient analog waveforms to more efficient digital waveforms, and the natural gaps in utilization that occur throughout the day due to variations in demand [8]-[9].

Consequently, the problem that needs to be confronted is the complexity and heterogeneity of the B3G environment, in combination with the scarcity and underutilization of the RF spectrum. *Cognitive radio* [10]-[11] appears as an effective, highly promising solution to this combined problem. Cognitive radio systems are able to sense their RF environment and react, either proactively or reactively, to external stimuli. By the term ‘react’ it is implied that the systems have the ability to reconfigure the algorithms and parameters of their operation, in order to better adapt to environment conditions. Thus, the operation of a typical cognitive radio system includes two stages: (a) *observe* and (b) *decide*. The first stage can be divided into two separate functional tasks: *sensing* and *reasoning*. Conclusively, as depicted in Figure 1, three fundamental functional tasks can be distinguished within a cognitive radio operational cycle: (i) *Sensing*: This involves

tuning to a frequency band and measuring the interference levels perceived. *(ii) Reasoning*: This encompasses the estimation of the capabilities of a candidate configuration, based on the levels of interference measured in task (i). *(iii) Decision-reaching*: Based on the estimations of task (ii), the most suitable configuration is selected, taking under consideration current traffic demands, as well as mobility and positioning patterns.

The present paper focuses on stage (a), and especially on functional task (ii) (reasoning). After briefly setting the scene, by concisely discussing the main principles/attributes of cognitive radio systems (Section II) and by outlining the ways in which functional task (i) (sensing) can be performed in a real-life cognitive radio system (Section III), the paper specifies a complete process for obtaining estimations of the capabilities of candidate configurations, in terms of transmission capacity and coverage range, based on the sensed levels of interference (Section IV). In the sequel, these estimations are enhanced by incorporating a machine learning technique (Section V). The motivation for this stems from the fact that a cognitive element's environment changes over time, thus it is difficult to estimate the capabilities of alternate configurations with a high degree of assurance. Finally, comprehensive results from the employment of the proposed machine learning technique are presented (Section VI), and concluding remarks are drawn (Section VII).

II. PRINCIPLES OF COGNITIVE RADIO

Cognitive radio is based upon the following main principles:

(a) Reconfigurability: This property of cognitive radios refers to their ability to dynamically modify their configuration. A *configuration* denotes a combination of RAT and spectrum. Different RATs support different (also, possibly more than one) parameters and algorithms for modulation, coding and error control.

Reconfigurability can efficiently be realized through the use of network (and terminal) elements (transceivers) that can dynamically alter the parameters of their operation, in order to improve the offered QoS. Reconfigurations are software-defined, i.e. they are carried out by activating the appropriate software at the transceiver.

As an example of this, let us assume a B3G cell comprising three reconfigurable network elements (transceivers) e_1 , e_2 and e_3 , each one capable of alternately operating in one of n configurations, namely c_1, c_2, \dots, c_n . During a specific time period, the best configuration, in terms of transmission capacity, coverage, mobility support and cost, might be configuration (c_1, c_3, c_2) . However, environmental conditions and requirements change dynamically, so in a next time period configuration (c_1, c_4, c_2) might be the most suitable one. In this example, element e_2 was reconfigured to operate under configuration c_4 instead of c_3 .

(b) Cognition: It is exactly this stochastic nature of the environment conditions that raises the need for the existence of the second main attribute of cognitive radio systems, i.e. cognition. Cognition refers to the ability of sensing the RF environment and extracting knowledge (data and experience) about the achievable capabilities of alternate configurations.

(c) Self-management: Although not inherent, this attribute can be incorporated into a cognitive radio system, with a view to rendering it more scalable [12]. In this sense, each transceiver should be able of *self*-adapting to its environment, without the need of being instructed by a central management entity with higher rationality. This concept, which is aligned to the *autonomic computing* paradigm, provides significant reduction of a system's complexity, since it does not call for a centralized management entity.

III. SENSING

Interference is one of the most restraining factors in the operation of cognitive radio. The

sensing task refers to the procedure of measuring the perceived levels of interference in a certain frequency band, in the area of interest. In order to quantify the effects of interference into signal transmission, two appropriate metrics can be employed: (a) the signal-to-interference-plus-noise ratio (SINR), represented by the ratio between the received wanted carrier signal power, and the total received interference power; and (b) the interference temperature (IT), T_I , represented by the ratio between the interference power, I , and the spectrum bandwidth, B , multiplied by the Boltzmann's constant, k , i.e.: $T_I = \frac{I}{kB}$. According to the Federal Communications Commission's (FCC) model [13] regarding IT, for a given frequency band in a given geographic location, an 'interference temperature limit', T_L , is defined by some regulatory agency. A transmitter should then ensure that, by transmitting, it does not raise the current IT above the specified IT limit [14], i.e.: $P_S / kB + T_I \leq T_L$, where P_S represents the transmit power.

Either of the two aforementioned metrics can be utilized by a cognitive radio system. A systematic sensing process involves instructing (part of) the local terminals to (a) temporarily switch to a different frequency band, (b) perform interference measurements, and (c) report them back to the network side. The latter can then be exploited by the network side (the reconfigurable transceiver), in conjunction with the attributes and characteristics of each *candidate RAT*, in order to reach estimations about each RAT's anticipated capabilities (expected performance) in the examined frequency band. In the near future, a major part of the research and standardization activities is expected to be targeting at producing the complete specifications of this sensing process.

IV. REASONING

After receiving the SINR or IT measurements from the terminals (downlink case), or

calculating itself the SINR or IT (uplink case), the network transceiver's management module is responsible for extracting conclusions about the capabilities of each candidate RAT in the frequency band under study. Due to the dynamic and stochastic nature of the environment conditions, it would be wiser to consider these estimations as *instantaneous estimations* (i.e., not fully reliable), which should be further enhanced by an appropriate mechanism (machine learning technique).

In what follows, we concentrate on how to reach instantaneous estimations about the transmission capacity (i.e., maximum achievable throughput) and the coverage range of a candidate configuration (combination of RAT and spectrum), based on the results of the sensing process. The analysis will be confined to the downlink case, yet the uplink case is similar. As input, a set of SINR values will be assumed. The analysis in case of IT values remains the same.

A. Transmission capacity

Depending on the candidate RAT, the measured SINR values can be mapped to maximum achievable bit-rates (throughputs), taking into account the specific characteristics (e.g., physical modes) of the RAT (Figure 2).

This can be clarified by considering the example of the IEEE 802.11b WLAN technology. 802.11b clients can operate at 11 Mbps (using QAM-64), but will scale back to 5.5 Mbps (QAM-16), 2 Mbps (QPSK), or 1 Mbps (BPSK), if signal quality becomes an issue. Since the lower data rates use less complex and more redundant methods of encoding the data, they are less susceptible to corruption due to interference and signal attenuation.

The network transceiver's management module uses, for each candidate RAT, a reference adaptive scheme, in order to map each input SINR value to a corresponding bit-rate value. Subsequently, it statistically processes the bit-rate values, in order to extract a metric that is

referred to as *effective transmission capacity*, as depicted in Figure 2. This metric expresses the anticipated average transmission capacity, with the term “average” implying that the metric has been calculated based on SINR reports from all the terminals involved in the sensing process. This computation may vary from being very simple (a typical average value) to more complicated (like Kalman filtering [19]). The goal is to take into account all measurements, not only the worst or the best cases, in order to gain a more realistic picture concerning the candidate configuration’s capabilities in terms of transmission capacity.

Back to the 802.11b example, if at a given moment 20% of the users can achieve a maximum bit-rate of 11 Mbps, 0% 5.5 Mbps, 30% 2 Mbps, and 50% 1 Mbps, then, by averaging this input, the effective transmission capacity can be estimated as $0.2 \cdot 11 + 0.3 \cdot 2 + 0.5 \cdot 1 = 3.3$ Mbps.

Formally, the process described above can be expressed as follows: Given the spectrum portion b under study and a candidate RAT r , it holds that:

$$cap_{ine}(r, b) = \frac{1}{N} \sum_{i=1}^N ABR(SINR_i(b), r) \quad (1)$$

where: $cap_{ine}(r, b)$ denotes the instantaneous value of the effective transmission capacity for the spectrum portion b under study and the candidate RAT r ; N indicates the number of terminals that took part in the sensing process; $SINR_i(b)$ denotes the SINR value measured by terminal i in the spectrum portion b ; and function $ABR(SINR_i(b), r)$ returns the achievable bit-rate value that corresponds to the input SINR value, $SINR_i(b)$, by employing the reference adaptive scheme of RAT r . In case some other form of statistical processing is used (e.g., Kalman filtering), then formula (1) should be substituted accordingly.

B. Coverage

The objective here is similar, i.e. to extract an instantaneous estimation about the *effective*

coverage range of a candidate RAT, in the frequency band under consideration. This metric expresses the anticipated average coverage range. Let it be noted that the effective coverage range does not represent the actual coverage area of the candidate configuration, but is rather a metric (grade) of the configuration's effectiveness in terms of coverage. The proposed process is depicted in Figure 3, and can be divided into two phases: In phase (a), the path loss exponent \hat{n} in the transceiver's area and the effective shadow loss $\hat{\sigma}$ are calculated. As implied by its name, the effective shadow loss $\hat{\sigma}$ expresses the anticipated average shadow loss experienced by all involved terminals. In phase (b), an instantaneous estimation about the effective coverage range is reached. The accuracy of estimating the path loss exponent and the shadow loss, in correlation with the number of collected measurements, is also discussed in [19]-[24].

In phase (a), the following input from each involved terminal is utilized: (i) the power of the desired signal (i.e., the power of the received training sequence, not including the interference power); and (ii) the terminal's location (distance from the transceiver). Concerning (ii), only the Global Positioning System (GPS) can provide adequate accuracy in location detection; however, the current trend for mobile terminals is to incorporate GPS receivers. After taking into account the input from all the involved terminals, an estimation of the path loss exponent \hat{n} and the effective shadow loss $\hat{\sigma}$ is reached, as illustrated in Figure 3.

In phase (b), the following input is utilized: (i) the path loss exponent and the effective shadow loss, as determined in phase (a); (ii) the minimum required SINR value in order to ensure acceptable quality (this value is RAT-dependent); (iii) the transmission power that has been used while taking the measurements (this value may also be RAT-dependent); and (iv) the mean interference power value, based on the reports of the involved terminals. By processing this input, an instantaneous estimation of the effective coverage range can be achieved.

Formally, the process described above can be expressed as follows:

Phase (a). It holds that:

$$rx_i = tx - 10n \log(d_i) - \sigma \quad (2)$$

where: rx_i represents the received power (expressed in dBm), by terminal i , of the desired signal, tx indicates the transmitted power (expressed in dBm) of the desired signal, n denotes the path loss exponent (expressed in dB), d_i is the distance between terminal i and the transceiver (expressed in m), and σ corresponds to the shadow loss (expressed in dB).

Estimates of the path loss exponent, \hat{n} , and the effective shadow loss, $\hat{\sigma}$, can be reached by employing linear regression. The results are summarized in what follows:

$$\hat{n} = \frac{N \cdot S_{XY} - S_X S_Y}{N \cdot S_{XX} - S_X S_X} \quad (3)$$

$$\hat{\sigma} = \frac{S_Y - \hat{n} \cdot S_X}{N} \quad (4)$$

where:

$$S_X = x_1 + x_2 + \dots + x_N, \quad S_Y = y_1 + y_2 + \dots + y_N,$$

$$S_{XX} = x_1^2 + x_2^2 + \dots + x_N^2, \quad S_{XY} = x_1 y_1 + x_2 y_2 + \dots + x_N y_N, \quad (5)$$

$$\text{and: } x_i = 10 \log(d_i), \quad y_i = tx - rx_i, \quad i = 1, 2, \dots, N \quad (6)$$

Phase (b). The minimum required SINR value, $SINR_{\min, req}$, for ensuring acceptable quality, together with the mean interference power, \bar{I} , as perceived by the involved users, can be used to compute the minimum required received power, $rx_{\min, req}$:

$$rx_{\min, req} = SINR_{\min, req} + \bar{I} \quad (7)$$

$$\text{where: } \bar{I} = \frac{1}{N} \sum_{i=1}^N I_i \quad (8)$$

with I_i denoting the interference power measured by terminal i . Hence, in order to compute an estimation, $d_{eff,ine}$, of the effective coverage range, the following equation must be solved:

$$rx_{\min,req} = tx - 10\hat{n} \log(d_{eff,ine}) - \hat{\sigma} \quad (9)$$

which results in:

$$d_{eff,ine} = 10^{\left(\frac{tx - rx_{\min,req} - \hat{\sigma}}{10\hat{n}}\right)} \quad (10)$$

Note that the values of tx and $SINR_{\min,req}$ are, in general, dependent on the RAT r under investigation.

V. INCORPORATING MACHINE LEARNING

A. The need for robustness

The instantaneous estimations reached through the procedures described in the previous section, concerning a candidate configuration's effective transmission capacity and coverage range, are by definition *instantaneous*. This is because these capabilities change frequently and randomly, since they are influenced by the varying environment conditions, including the configuration selections of “near-by” autonomous network transceivers.

As a response to this problem, functional task (ii) (reasoning) needs to be enhanced by a machine learning technique. This section proposes a computationally efficient technique, the goal of which is twofold:

(a) to smooth out any fluctuations originating from momentary conditions which do not reflect the actual situation of the RF environment; this can be achieved by taking into account past knowledge (experience).

(b) to render the system adaptable to the permanent changes, by taking under consideration the

recent instantaneous estimations.

For this purpose, the proposed technique makes use of *Bayesian Networks*, which constitute an advanced and extensible method of modelling and reasoning about probabilistic relationships [15]-[18]. In conjunction with the deployment of a Bayesian Network, a simple *learning and adaptation strategy* is developed and employed, catering to keeping the knowledge encoded in the Bayesian Network up-to-date. We use the term *robust estimations* (i.e., stable and reliable) to distinguish the results of the employed machine learning method from the *instantaneous estimations*.

B. Bayesian model

Figure 4(a) depicts the basic Bayesian Network that is proposed for modelling the problem at hand. The randomness and uncertainty of a candidate configuration's capabilities (effective transmission capacity and effective coverage range) leads us to the employment of corresponding random variables, as depicted in Figure 4(a), where *CAP* corresponds to effective transmission capacity, *COV* to effective coverage range, and *CFG* to configuration.

Each of the aforementioned random variables can take a value from a set of discrete possible values (the denser/larger the grid of possible values the more accurate the results). Given a candidate configuration c (i.e., given that $CFG=c$), and based on the network transceiver's past experience, the possible values of *CAP* are not (at least not in general) equally probable (the same applies for the possible values of *COV*).

In order to express this, a number of Conditional Probability Tables (CPTs) is organized, as depicted in Figure 4(a) (only the CPTs for *CAP* are shown, to save space). Each CPT refers to a particular candidate RAT. Let R denote the set of RATs that our reconfigurable network transceiver supports, then $2^{|R|}$ CPTs in total are required for the full information (both for *CAP*

and COV). Each column of a CPT refers to a specific configuration (i.e., RAT and carrier frequency). Each line of the CPT corresponds to a possible value of either CAP or COV . Each cell (intersection of line and column) provides the probability that the configuration (corresponding to the column) will achieve the potential CAP or COV value (corresponding to the line). Given a configuration, the most probable value of CAP is the value that corresponds to the maximum conditional probability. The same applies for the most probable value of COV . The most probable values of CAP and COV , given a specific configuration, constitute the *robust estimations* of the effective transmission capacity and the effective coverage range, for this configuration, respectively.

Let us focus on the CPT for CAP of an arbitrary RAT r_l ($r_l \in R$). With F denoting the set of spectrum carriers with which RAT r_l may operate, the CPT consists of $|F|$ columns ($|F|$ representing the size of set F), corresponding to configurations (combinations of RAT and spectrum carrier) $c_1=(r_l, f_1), \dots, c_{|F|}=(r_l, f_{|F|})$. With V denoting the set of potential values supported by RAT r_l , the CPT consists of $|V|$ lines, corresponding to CAP values $cap_1, cap_2, \dots, cap_{|V|}$. Without loss of generality, enumeration is done in ascending order, i.e. $cap_1 < cap_2 < \dots < cap_{|V|}$, so $cap_{|V|}$ is the maximum possible value. The cell located at the intersection of line i and column j is a conditional probability value. It expresses the probability that effective transmission capacity cap_i will be achieved, if configuration c_j is selected. Formally, this is denoted as $\Pr[CAP = cap_i | CFG = c_j]$. For COV , we use the symbol W in place of V . Also, note that, for notational simplicity, we write F , instead of F_{r_l} . The same applies for sets V and W . Let it be noted, however, that sets F , V , and W are, in general, different for every $r \in R$.

C. Learning and adaptation strategy

Initially, the probability values contained in the CPTs of the Bayesian Network are nothing

more than reference values that have been defined either randomly or, in the best case, by a set of experts. However, this is not sufficient. These values must be constantly updated, by incorporating knowledge and experience gained from both the past and the most recent instantaneous estimations.

In order to achieve this, a computationally efficient learning and adaptation strategy is proposed, which determines how the CPT values should be updated. Figure 4(b) is a block diagram of the proposed strategy. We will focus on an arbitrary configuration $c=(r, f)$ and examine how the update is performed on the corresponding probability values of the CPT for CAP . The strategy followed for COV is exactly the same.

Let cap_{ine} denote the value of the most recent instantaneous estimation about the effective transmission capacity of configuration c (cap_{ine} is a continuous, i.e. not discrete, variable). The update process takes into account the “distance” (absolute difference) between each candidate CAP value and the value of cap_{ine} . Depending on this distance, each CPT value that corresponds to the configuration under consideration should be properly increased or decreased.

For this purpose, a correction factor cor_i is computed for each candidate CAP value cap_i . It holds that $0 \leq cor_i \leq 1$. A value close to 1 reflects that the corresponding candidate value cap_i is close to the instantaneous estimation cap_{ine} , and thus it should be reinforced accordingly. The opposite stands for a value that is close to 0. Formally, the correction factor cor_i is expressed as follows (Figure 4(b)):

$$cor_i = 1 - \frac{|cap_i - cap_{ine}|}{cap_{max}} \quad (11)$$

where: $cap_{max} = \max(cap_{|V|}, cap_{ine})$

Subsequently, the new value of each conditional probability, $\Pr[CAP = cap_i | CFG = c]$, is

computed as the product of the old conditional probability value, the corresponding correction factor, and a normalizing constant L . The parameter of this normalizing constant is computed by requiring all the “new” probabilities to sum up to 1. This can be formally denoted as:

$$\Pr[CAP = cap_i | CFG = c]_{new} = L \cdot cor_i \cdot \Pr[CAP = cap_i | CFG = c]_{old} \quad (12)$$

We state that the system has converged when the most probable candidate CAP value (i.e., the one that corresponds to the maximum conditional probability) is closer, than any other candidate CAP value, to the instantaneous estimation’s value, cap_{ine} . After convergence, we limit the number U of consecutive updates that can be applied to the conditional probabilities of the specific configuration to a maximum U_{max} . This is a practical mechanism that assists in accomplishing faster adaptation to new conditions.

For the same reason, we do not permit the value of a conditional probability to fall under a certain threshold, denoted as *threshold*. The value of this parameter is determined as $threshold = A/|V|$, where $0 < A < 1$ ($|V|$ is the number of potential CAP values). In cases where the threshold mechanism has to be applied, the normalizing constant L is computed by requiring all the other “new” probabilities to sum up to $1 - K \cdot threshold$, where K is the number of probabilities that have been assigned equal to the threshold. The values of U_{max} and A are design parameters.

VI. RESULTS

In this section, two comprehensive scenarios are presented, demonstrating the functionality of the proposed machine learning technique.

A. Scenario 1

In this scenario, we will focus on an arbitrary configuration $c_l = (r_l, f_l)$ and examine how the

update is performed on the corresponding probability values of the CPT for CAP . The method followed for COV does not differ.

The values of the scenario's parameters are depicted in Figure 5(a). We assume there are $|V|=5$ candidate (potential) CAP values, namely (in Mbps): $cap_1=0.4$, $cap_2=0.8$, $cap_3=1.2$, $cap_4=1.6$, $cap_5=2.0$. Note that, in general, the candidate CAP values need not be equally distant. We will examine 6 time periods, namely periods 0 through 5. Figure 5(b) (first two columns) indicates how the values of the instantaneous estimation cap_{ine} evolve. In particular, in the first two time periods, $cap_{ine}=0.96$, while, in the next three, $cap_{ine}=1.68$ (in Mbps). In the following, we use the notation $cap_{ine}(0)$, $cap_{ine}(1)$, and so on, to distinguish among the different values of cap_{ine} , through the time periods 0, 1, etc., respectively.

The expected behaviour of the model is to initially select $cap_2=0.8$ as the most probable value, since it is closer to 0.96, and then *gradually and not instantly* converge to $cap_4=1.6$ (which is the closest value to 1.68). This gradual convergence constitutes a fundamental requirement concerning the model's functionality, since it is not known in advance whether the "new" cap_{ine} value, i.e. the value 1.68, represents a temporary or permanent environment situation.

Figure 5(c) illustrates the distribution of the conditional probabilities through the various time periods of the scenario. Initially (*period 0*), all candidate values are considered equally probable, thus the distribution is uniform, and any value can be considered as the most probable one. Subsequently, the value of cap_{ine} in *period 0*, i.e. the value $cap_{ine}(0)$, together with the probability distribution of *period 0*, are taken into account in order to compute the probability distribution of *period 1*. The same procedure is followed for all periods, i.e. the probability distribution of *period N*, in conjunction with $cap_{ine}(N)$, serve as input for the computation of the probability distribution of *period N+1*, following the machine learning method specified in Section V.

As can be observed from Figure 5(b) and Figure 5(c), cap_2 is correctly selected in *period 1* as the most probable *CAP* value. As was expected for this period, there are high values for cap_2 and cap_3 , a slight diminishment for cap_1 and cap_4 , and a severe degradation for cap_5 . In *period 2*, the scheme is further applied, and since $cap_{ine}(1)$ is equal to $cap_{ine}(0)$, the most probable value does not change and is actually further reinforced. However, during *period 2* the value of cap_{ine} changes, and more specifically becomes equal to $cap_{ine}(2)=1.612$. Thus, in the next time period, i.e. *period 3*, cap_3 is selected as the most probable value. It is important to notice at this point that, although cap_4 is closer to $cap_{ine}(2)$, nonetheless cap_3 (instead of cap_4) is chosen as the most probable value. This constitutes the desired behaviour, i.e. to adapt gradually and not immediately, in order to avoid oscillations and smooth out temporary fluctuations. In the following time period, *period 4*, cap_3 remains the most probable value, but cap_4 is also reinforced considerably. Then, in *period 5*, the model converges to cap_4 , since the value of cap_{ine} has remained the same (equal to 1.68) for a considerable amount of time. Finally, we may also note from Figure 5(c) that, in the last two periods, the probability of cap_1 has been set equal to the threshold's value, i.e. equal to $A/|V| = 0.02$.

B. Scenario 2

Scenario 2 aims at illustrating more thoroughly *how the proposed system avoids temporary fluctuations and converges to permanent changes*. We will focus on an arbitrary configuration $c_2 = (r_2, f_2)$ and examine how the update is performed on the corresponding probability values of the CPT for *CAP*. The values of the scenario's parameters are depicted in Table I. We assume that there are $|V|=6$ candidate (potential) *CAP* values, namely (in Mbps): $cap_1=6$, $cap_2=12$, $cap_3=24$, $cap_4=36$, $cap_5=48$, $cap_6=54$. In this scenario, we simulate various different cases. For all cases, a uniform distribution is assumed as the starting point (*period 0*).

Case A1. The values of the instantaneous estimation cap_{ine} evolve as follows (Table II): $\{7, 7, 7, 11, 7, 7, 7, 7, \dots\}$, i.e. in the first three time periods (*periods 0-2*) cap_{ine} is 7 Mbps, then in *period 3* we have a temporary change (11 Mbps), and thereafter cap_{ine} is again equal to 7 Mbps. Figure 6(a) depicts the system's behaviour in this case. As may be observed, in *period 4*, the (probability of the) 12 Mbps candidate value gains some ground, yet the 6 Mbps value remains the most probable one, which constitutes the desired behaviour, i.e. to adapt gradually and carefully to new conditions, avoiding temporary fluctuations.

Case A2. The values of the instantaneous estimation cap_{ine} evolve as follows (Table II): $\{7, 7, 7, 11, 11, 11, 7, 7, 7, 7, \dots\}$. Figure 6(b) depicts the system's behaviour in this case. As may be observed, in *period 6*, the 12 Mbps value manages to almost outperform the 6 Mbps value. In *period 7*, the system does not further reinforce the 12 Mbps value, since $cap_{ine}(6)=7$.

Case A3. The values of the instantaneous estimation cap_{ine} evolve as follows (Table II): $\{7, 7, 7, 11, 11, 11, 11, 11, 11, 7, 7, 7, 7, \dots\}$. Figure 6(c) depicts the system's behaviour in this case. This time, the 12 Mbps value becomes the most probable one, in *period 7* (taking an overall of 4 time periods for the system to converge). In *period 10*, the 12 Mbps value starts to degrade, since $cap_{ine}(9)=7$. In *period 13*, the system adapts back to the 6 Mbps value.

Case A4. The values of the instantaneous estimation cap_{ine} evolve as follows (Table II): $\{7, 7, 7, 11, 11, 11, 11, 11, 11, 11, \dots\}$. As can be deduced, we now consider a permanent change in the environment conditions. Figure 6(d) depicts the system's behaviour in this case. Within 4 time periods (*periods 4-7*), the system adapts to the new situation, and as the scheme is further applied, the 12 Mbps value is further reinforced.

Cases B1 – B4. For each of these cases, the values of the instantaneous estimation cap_{ine} evolve as depicted in Table III. In case B1 (Figure 7(a)), the 12 Mbps value approaches, in

period 4, the 6 Mbps value, which remains, however, the most probable one. Thus, in case B1, the system completely avoids the fluctuation. In case B2 (Figure 7(b)), the system makes one step towards the 24 Mbps value, by selecting the 12 Mbps value as the most probable one, for *periods 5-8*. As may be observed, although $cap_{ine}(6)=7$, the system does not immediately return to the 6 Mbps value, since this may be a temporary fluctuation as well. Instead, it stays on the 12 Mbps value for two more periods (*periods 7-8*), and then falls back to the 6 Mbps value. Conclusions are essentially the same for case B3 (Figure 7(c)), the only differences being, as expected, that the system stays longer on the 12 Mbps value (*periods 5-11*), and that the 24 Mbps value is reinforced until *period 7*. In case B4 (Figure 7(d)), in which we consider a permanent change, we may observe that the system finally converges to the 24 Mbps value in *period 10*.

Cases C1 – C4. For each of these cases, the values of the instantaneous estimation cap_{ine} evolve as depicted in Table IV. In essence, we have a similar situation with cases B1 – B4. In case C1 (Figure 8(a)), the 6 Mbps value continues to remain the most probable one, even in *period 4*. In case C2 (Figure 8(b)), the system firstly adapts to the 12 Mbps value (*period 5*), and then to the 24 Mbps value (*period 6*), before falling back again to the 12 Mbps value (*period 9*) and then gradually back to the 6 Mbps value. In case C3 (Figure 8(c)), the system stays longer on the 24 Mbps value, before falling back towards lower expected capacity values. Finally, case C4 (Figure 8(d)) illustrates that the system converges to the 36 Mbps value in *period 14*.

Discussion. In general, a learning strategy aims at simulating the behaviour of a rational supervisor of the system that has the ability to observe a sequence of system-related events. In this sense, the adaptation procedure followed in the proposed scheme puts effort in imitating the behaviour of such a supervisor. Thus, a person observing a series of events within a highly

“noisy” environment, meaning that the observed event may not reflect the actual conditions, has some reservations about the certainty of the observations. This yields a “waiting” period during which the observer wishes to record additional events, before reaching a conclusion. This is exactly what the presented Bayesian model tries to approximate. An experienced system supervisor can often make faster, more intuitive decisions, based on his/her experience, avoiding hysteresis, i.e. slow reaction. On the other hand, although a learning model is able to reach optimum results, this may come at the cost of a hysteresis, something which is inherent to most automated decision-making mechanisms.

VII. CONCLUSIONS AND FUTURE WORK

Despite being a relatively recent concept, cognitive radio is rapidly advancing and is considered today as a highly promising way towards handling the complexity of the B3G wireless scenery. Cognitive radio systems dynamically reconfigure the algorithms and parameters they use, in order to adapt to the changing environment conditions. However, making proper reconfiguration decisions presupposes a way of knowing, with high enough assurance, the capabilities of the alternate configurations, especially in terms of achievable transmission capacity and coverage.

For this purpose, the present paper firstly focused on specifying a complete process for obtaining instantaneous estimations of the capabilities of candidate configurations, in terms of transmission capacity and coverage. In the sequel, it concentrated on enhancing these estimations, by employing a machine learning technique, based on Bayesian Networks, in conjunction with an effective learning and adaptation strategy. Comprehensive results were presented, in order to validate the functionality of the proposed method. Next phases of our work involve focusing on the decision-reaching task of cognitive radio, and more specifically on the

determination of the most suitable configuration, taking under consideration the configurations' capabilities, as well as traffic demand predictions, user mobility and location patterns, and cost. Another potentially interesting issue is to examine how data pertaining to the network (e.g., traffic load) and how data pertaining to the terminal devices themselves (e.g., remaining battery life, transmission or signal filtering capabilities) can be combined in order to facilitate the estimation of the best reconfiguration choice.

ACKNOWLEDGEMENT

This work has been performed in the framework of the ARIADNE project (03ED235), partially funded by the General Secretariat of Research and Technology (GSRT) of the Greek Ministry of Development. Work of P. Demestichas is also conducted and funded in the framework of the European Integrated IST project E2R II.

REFERENCES

- [1] "Management of heterogeneous networks", *feature topic in the IEEE Communications Magazine*, Vol. 36, No. 3, March 1998.
- [2] "Fourth generation wireless networks and interconnecting standards", *Special Issue in the IEEE Personal Communications*, Vol. 8, No. 5, Oct. 2001.
- [3] Y. Kim, B. J. Jeong, J. Chung, C.-S. Hwang, J. S. Ryu, Ki-Ho Kim, and Y. K. Kim, "Beyond 3G: Vision, Requirements, and Enabling Technologies", *IEEE Commun. Mag.*, Vol. 41, No. 3, pp. 120-124, Mar. 2003.
- [4] P. Demestichas, G. Vivier, K. El-Khazen, M. Theologou, "Evolution in wireless systems management concepts: from composite radio to reconfigurability", *IEEE Communications Magazine*, Vol. 42, No. 5, May 2004
- [5] M. McHenry, "Frequency agile spectrum access technologies", in *FCC Workshop Cognitive Radio*, May 2003.
- [6] G. Staple and K. Werbach, "The end of spectrum scarcity", *IEEE Spectrum*, Vol. 41, No. 3, pp. 48-52, March 2004.
- [7] S. Haykin, "Cognitive Radio: Brain-Empowered Wireless Communications", *IEEE JSAC*, Vol. 23, No. 2, pp. 201-220, Feb. 2005.
- [8] J. O'Daniell Neel, "Analysis and Design of Cognitive Radio Networks and Distributed Radio Resource Management Algorithms", Dissertation submitted to the Faculty of the Virginia Polytechnic Institute and State University in partial fulfilment of the requirements for the degree of PhD in Electrical Engineering, Blacksburg, VA, Sept. 2006.
- [9] M. McHenry, "NSF Spectrum Occupancy Measurements Project Summary", Aug. 15, 2005. Available online at: http://www.sharedspectrum.com/?section=nsf_measurements.
- [10] J. Mitola and G. Maguire Jr., "Cognitive Radio: Making Software Radios More Personal", *IEEE Personal Communications Magazine*, Vol. 6, No. 6, pp. 13-18, Aug. 1999.
- [11] J. Mitola, "Cognitive radio: An integrated agent architecture for software defined radio", Doctor of Technology, Royal Institute of Technology (KTH), Stockholm, Sweden, 2000.
- [12] P. Demestichas, D. Bosovic, V. Stavroulaki, Al Lee, and J. Strassner, "m@ANGEL: Autonomic Management Platform for Seamless Cognitive Connectivity to the Mobile Internet", *IEEE Communications Magazine*, Vol. 44, No. 6, pp. 118-127, June 2006.
- [13] Federal Communications Commission, "Establishment of interference temperature metric to quantify and manage interference and to expand available unlicensed operation in certain fixed mobile and satellite frequency bands", *ET Docket 03-289*, Notice of Inquiry and Proposed Rulemaking.
- [14] P. J. Kolodzy, "Interference temperature: a metric for dynamic spectrum utilization", *International Journal of Network Management, Special Issue: Management of Interference in Wireless Networks*, John Wiley & Sons, Vol. 16, No. 2, pp. 103-113, March 2006.
- [15] R. E. Neapolitan, "Learning Bayesian Networks – Series in Artificial Intelligence", *Prentice Hall*, 2002.
- [16] E. Adamopoulou, K. Demestichas, A. Koutsorodi, and M. E. Theologou, "Access Selection and User Profiling in Reconfigurable Terminals", in *Proc. of the 15th Wireless World Research Forum (WWRF)*, Paris, Dec. 2005.
- [17] A. Koutsorodi, E. Adamopoulou, K. Demestichas, and M. Theologou, "Service Configuration and User Profiling in 4G Terminals", *Wireless Personal Communications*, Springer, 0929-6212 (Print) 1572-834X (Online), May 2007.

- [18] J. Cheng and R. Greiner, "Learning Bayesian belief network classifiers: algorithms and system", in *Proc. of the 14th Canadian Conference on Artificial Intelligence*, pp. 141-151, 2001.
- [19] K. K. Leung, "Power control by interference prediction for broadband wireless packet networks", *IEEE Trans. Wireless Commun.*, Vol. 1, No. 2, pp. 256-265, Apr. 2002.
- [20] F. Santucci, M. Pratesi, M. Ruggieri, and F. Graziosi, "A general analysis of signal strength handover algorithms with cochannel interference", *IEEE Trans. Commun.*, Vol. 48, No. 2, pp. 231-241, Feb. 2000.
- [21] S. C. Schwartz and Y. S. Yeh, "On the distribution function and moments of power sums with lognormal components", *Bell Syst. Tech. J.*, Vol. 61, pp. 1441-1462, Sept. 1982.
- [22] M. Pratesi, M. Ruggieri, F. Graziosi, and F. Santucci, "Performance of signal strength handover algorithms with interference and correlated shadowings," in *Proc. IEEE Vehicular Technology Conf.*, Phoenix, AZ, pp. 530-534, May 1997.
- [23] F. Graziosi, M. Pratesi, M. Ruggieri, and F. Santucci, "A multicell model of handover initiation in mobile cellular networks," *IEEE Trans. Veh. Technol.*, Vol. 48, May 1999, pp. 802-814.
- [24] N. A. Marlow, "A Normal Limit Theorem for Power Sums of Normal Random Variables", *Bell Syst. Tech. J.*, Vol. 46, No. 9, pp. 2081-2089, 1967.

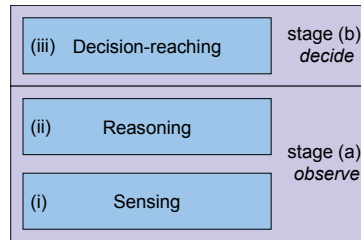


Figure 1: Functional tasks of cognitive radio operation

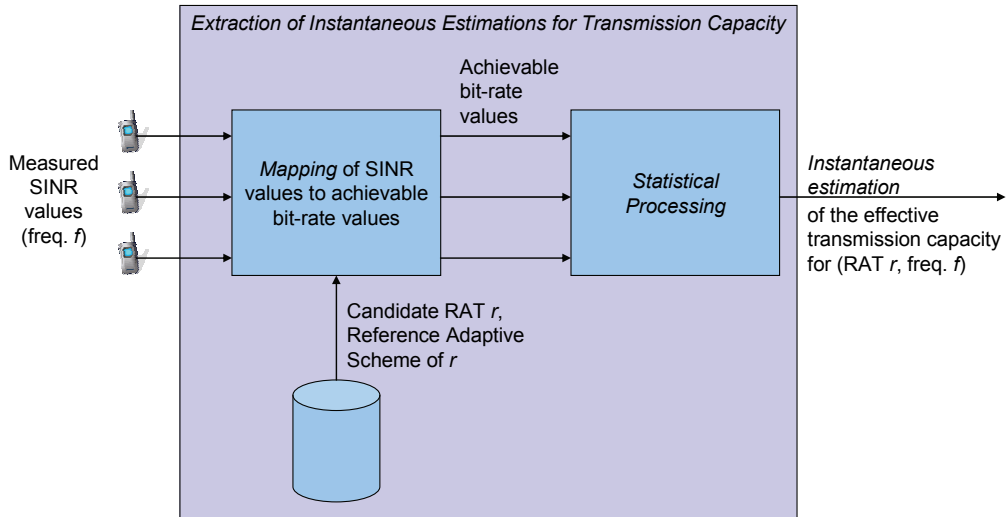


Figure 2: Process of extracting instantaneous estimations for the effective transmission capacity of a candidate configuration

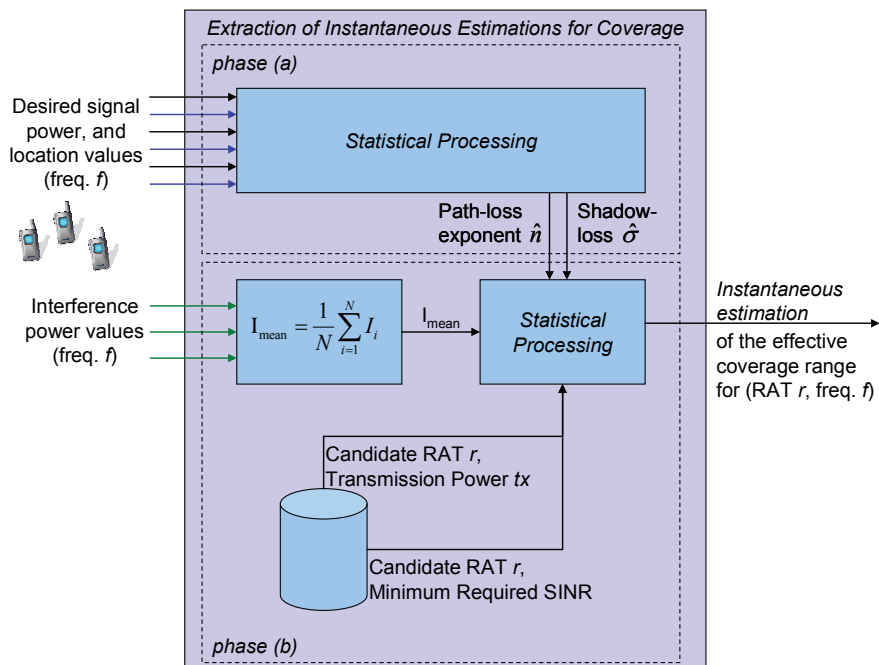


Figure 3: Process of extracting instantaneous estimations for the effective coverage range of a candidate configuration

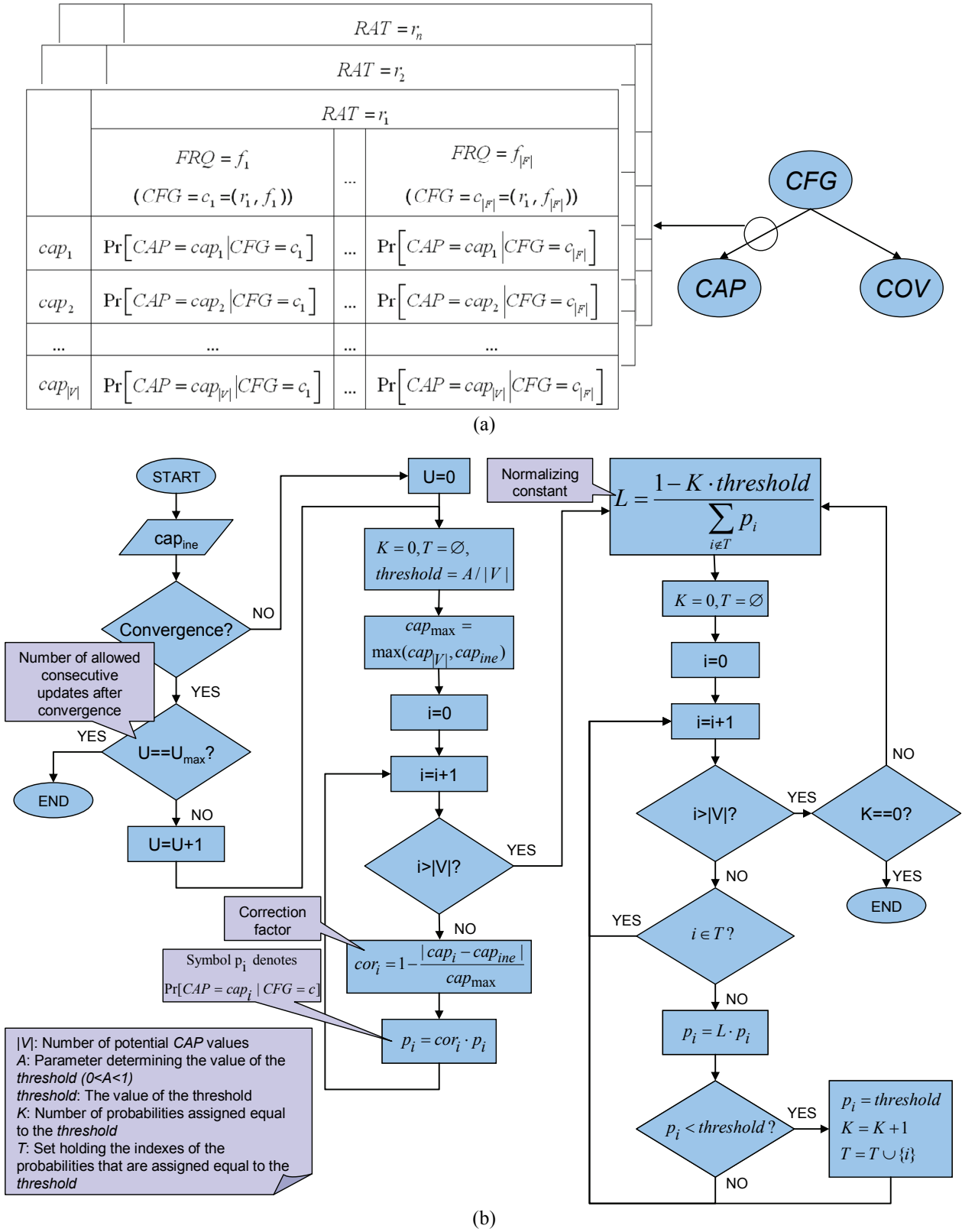


Figure 4: The proposed machine learning technique: (a) the deployed Bayesian Network; (b) the learning and adaptation strategy

Parameter	Description	Value
$ V $	number of potential <i>CAP</i> values	5
U_{max}	maximum number of consecutive updates after convergence	3
A	parameter for the determination of the <i>threshold</i>	0.1

(a)

Time Period	cap_{ine} (in Mbps)	Most probable <i>CAP</i> value
0	0.96	Any
1	0.96	0.8Mbps (cap_2)
2	1.68	0.8Mbps (cap_2)
3	1.68	1.2Mbps (cap_3)
4	1.68	1.2Mbps (cap_3)
5	...	1.6Mbps (cap_4)
...

(b)

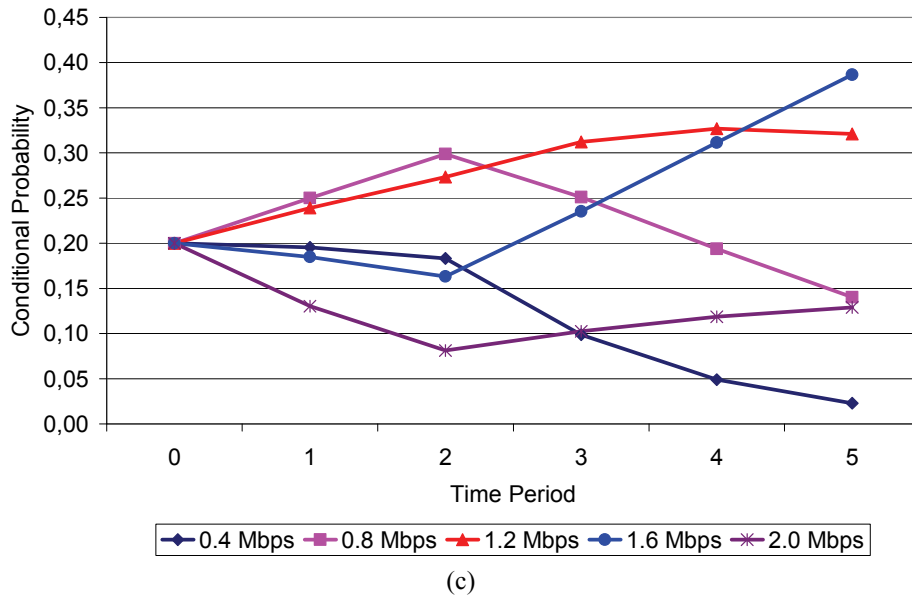


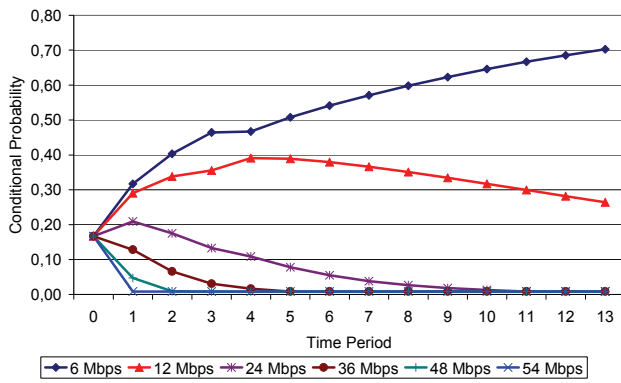
Figure 5: Scenario 1: (a) parameters of the scenario; (b) evolution of the instantaneous estimation's values and of the most probable *CAP* values; (c) evolution of the probability distribution

Table I: Parameters of Scenario 2

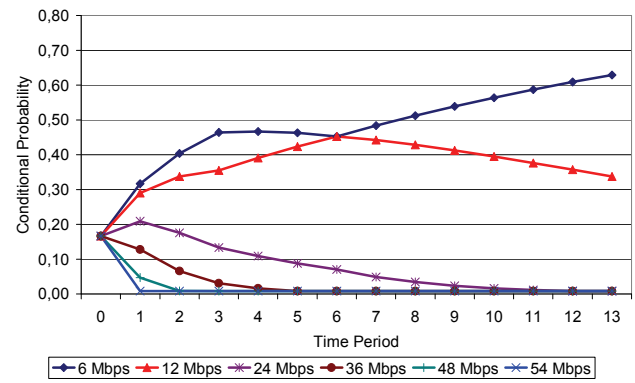
Parameter	Description	Value
$ V $	number of potential <i>CAP</i> values	6
U_{max}	maximum number of consecutive updates after convergence	3
A	parameter for the determination of the <i>threshold</i>	0.05

Table II: Scenario 2A – Evolution of the values of the instantaneous estimation cap_{ine}

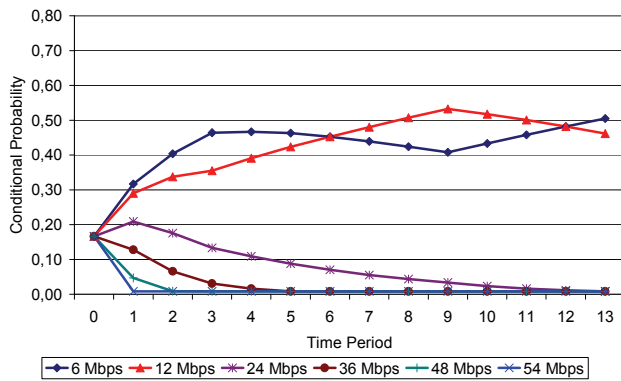
Time Period	cap_{ine} (in Mbps)			
	Case A1	Case A2	Case A3	Case A4
0	7	7	7	7
1	7	7	7	7
2	7	7	7	7
3	11	11	11	11
4	7	11	11	11
5	7	11	11	11
6	7	7	11	11
7	7	7	11	11
8	7	7	11	11
9	7	7	7	11
10	7	7	7	11
11	7	7	7	11
12



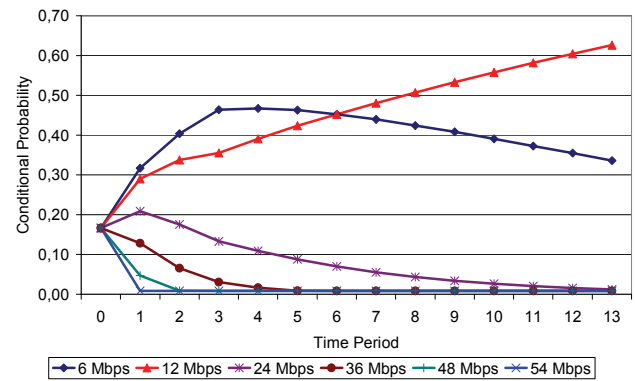
(a)



(b)



(c)

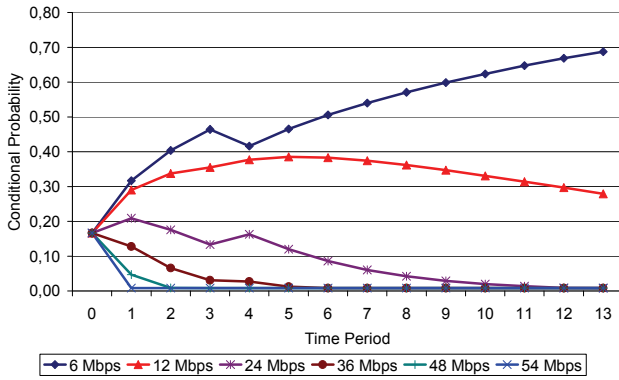


(d)

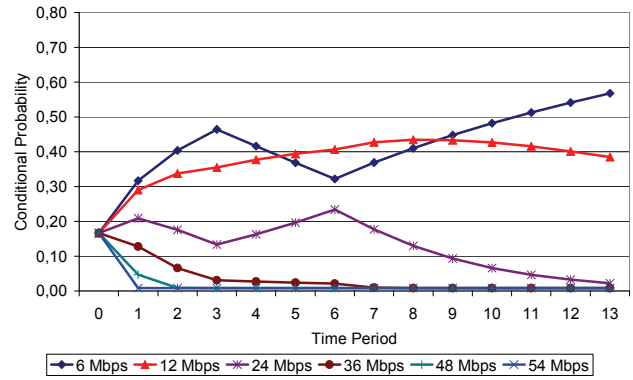
Figure 6: Scenario 2A – Evolution of the probability distribution in (a) case A1; (b) case A2; (c) case A3; and (d) case A4

Table III: Scenario 2B – Evolution of the values of the instantaneous estimation cap_{ine}

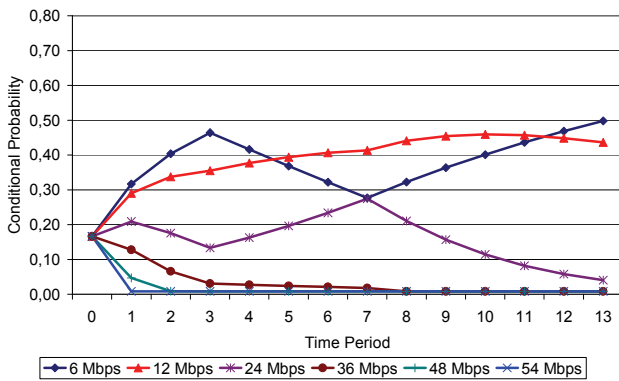
Time Period	cap_{ine} (in Mbps)			
	Case B1	Case B2	Case B3	Case B4
0	7	7	7	7
1	7	7	7	7
2	7	7	7	7
3	21	21	21	21
4	7	21	21	21
5	7	21	21	21
6	7	7	21	21
7	7	7	7	21
8	7	7	7	21
9	7	7	7	21
10	7	7	7	21
11	7	7	7	21
12



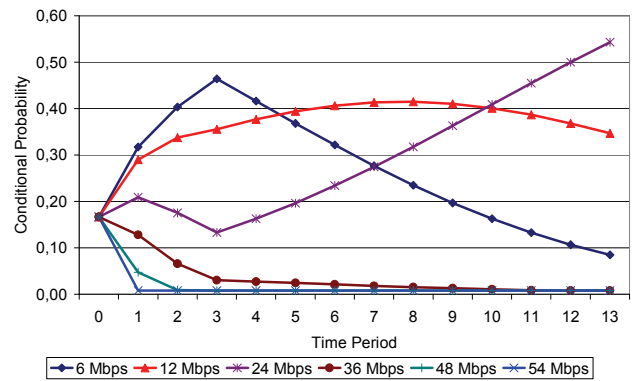
(a)



(b)



(c)

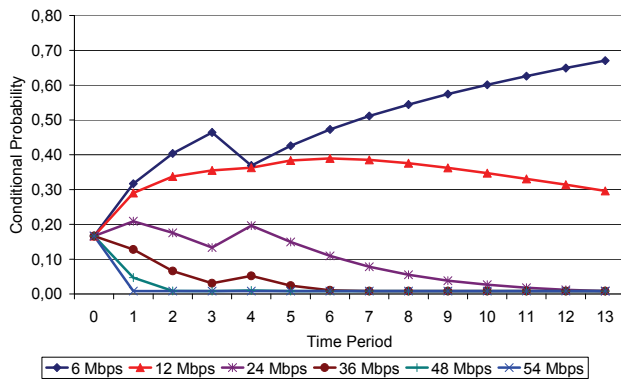


(d)

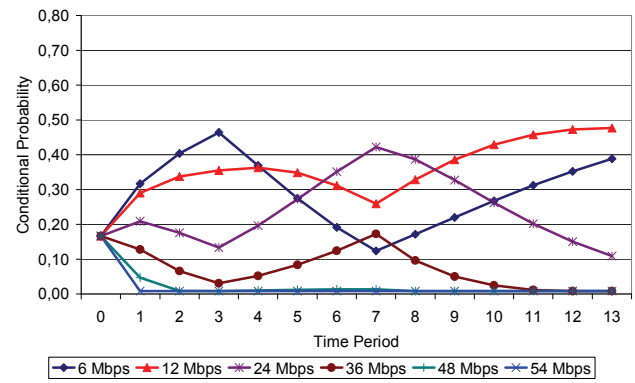
Figure 7: Scenario 2B – Evolution of the probability distribution in (a) case B1; (b) case B2; (c) case B3; and (d) case B4

Table IV: Scenario 2C – Evolution of the values of the instantaneous estimation cap_{ine}

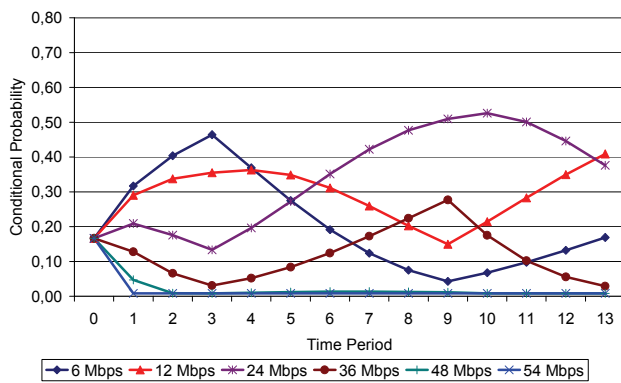
Time Period	cap_{ine} (in Mbps)			
	Case C1	Case C2	Case C3	Case C4
0	7	7	7	7
1	7	7	7	7
2	7	7	7	7
3	33	33	33	33
4	7	33	33	33
5	7	33	33	33
6	7	33	33	33
7	7	7	33	33
8	7	7	33	33
9	7	7	7	33
10	7	7	7	33
11	7	7	7	33
12



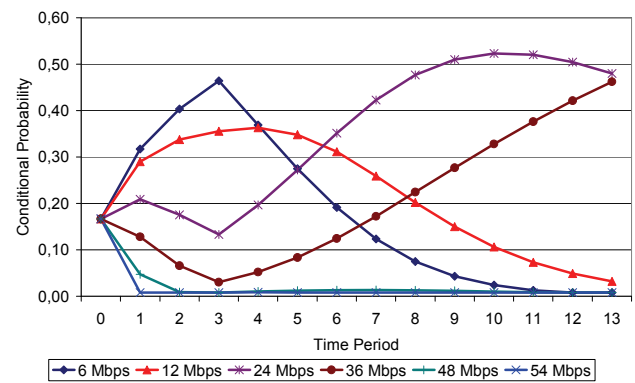
(a)



(b)



(c)



(d)

Figure 8: Scenario 2C – Evolution of the probability distribution in (a) case C1; (b) case C2; (c) case C3; and (d) case C4